Applied Clay Science 247 (2024) 107201

Contents lists available at ScienceDirect

Applied Clay Science

journal homepage: www.elsevier.com/locate/clay

Research Paper

A novel insight of interaction mechanism of carboxymethyl cellulose with talc surface: A combined molecular dynamic simulation and DFT investigation

Weiquan Zhan [a,b,c], Siyuan Yang [a,b,d], Shenxu Bao [a,b,d], Liuyi Ren [a,b,d], Cheng Liu [a,b,d,*]

[a] School of Resources and Environmental Engineering, Wuhan University of Technology, Wuhan 430070, China
[b] Key Laboratory of Green Utilization of Critical Non-metallic Mineral Resources of Ministry of Education, Wuhan, Hubei 430070, China
[c] Instituto de Fisica, Universidad Autonoma de San Luis Potosi, Av. Manuel Nava 6, Zona Universitaria, C.P. 78290, San Luis Potosi, S.L.P., Mexico
[d] Hubei Key Laboratory of Mineral Resources Processing and Environment, Wuhan University of Technology, Wuhan, Hubei 430070, China

ARTICLE INFO

Keywords:
Talc surface
CMC
MDs
DFT calculation
Interaction mechanism

ABSTRACT

Separation of talc from sulfide minerals through adding depressor in flotation field is very necessary, while the interaction of depressor on the surface of talc still needs to be further explained. Here, a typical depressor, carboxymethyl cellulose (CMC), interacted with talc surface was deeply investigated from atomic structure and surface hydration though molecular dynamic simulation (MDs) and density functional theory (DFT) calculation. MDs was applied on investigating adsorption behaviors of CMC on basal and edge plane of talc in aqueous solutions, and DFT was used for studying the interacted orbitals and charge transfer. It was found that adsorption of CMC on surface of edge plane was stronger than that on the surface of basal plane due to the enhanced interaction of polar group on the edge plane and the dragged water molecules. Interactions existed between H atoms in CMC and O atoms in edge plane, between O atoms in CMC and Si, Mg atoms in edge plane. The strong interacted water molecules dragged CMC close to the surface, thus to strengthen the binding of CMC and edge plane of talc. Furthermore, the hydration shell on the basal and edge plane of talc was investigated for explaining the phenomenon. Therefore, our work gave a new insight into the microscopic interaction between talc and CMC, thus to guide the actual application.

1. Introduction

Talc is a Mg-containing TOT type silicate mineral with the chemical formula of $(Mg_3(Si_2O_5)_2(OH)_2)$(Zhan et al., 2019; C. Li et al., 2021b; Burkett et al., 2022), the unit layer composition of two layers of silica tetrahedron held together with magnesium-oxygen octahedron, and magnesium ion is filled in the octahedral void with a coordination number of 6(Zhao et al., 2019; Chen et al., 2022). Talc is mainly cleaved along the basal plane due to the layered structure in the grinding process, meanwhile, talc flakes break easily due to the extremely low hardness, then forming edge plane(Liu et al., 2014; Yan et al., 2013; Zeitler et al., 2014). The basal plane of talc has no charged groups while the edge plane of that has charged ions (Mg^{2+} and OH^-)(Fuerstenau et al., 1988; Mälhammar, 1990; Atluri et al., 2018), it is believed that talc basal plane are hydrophobic and edge planes are probably be hydrophilic. Because of the special surficial properties, talc was widely applied in the field of heavy metal removal(Sprynskyy et al., 2011), dye wastewater adsorption(S. Chen et al., 2023a, 2023b), and catalyst carrier(Zafari et al., 2021). For instance, -SiOH and -MgOH groups as Brønsted acidic sites can be applied as carrier for construction of heterogeneous catalyst(Maleki et al., 2017; Dias et al., 2020).

The surface properties are depended on the ratio of basal plane to edge planes(Shortridge et al., 2000; Khraisheh et al., 2005) reported that the basal plane occupied 69% in an agglomeration of fine crystals of talc. Morris et al.(Morris et al., 2002) also reported a significant proportion of total talc surface was the basal plane. Hence, talc exhibits a natural hydrophobicity. Commonly, talc commonly associates with sulfide minerals in ore deposits, from pentlandite(Long et al., 2022), chalcopyrite to molybdenite(C. Li et al., 2021b; Zhong et al., 2021; Xian et al., 2022). Talc easily accesses the concentrate due to its surface hydrophobicity during the flotation process of sulfide minerals, then affecting the quality of concentrate(Luo et al., 2022b; Li et al., 2023). Besides,

* Corresponding author at: School of Resources and Environmental Engineering, Wuhan University of Technology, Wuhan 430070, China.
E-mail address: liucheng309@whut.edu.cn (C. Liu).

https://doi.org/10.1016/j.clay.2023.107201
Received 23 August 2023; Received in revised form 6 October 2023; Accepted 1 November 2023
Available online 8 November 2023

hydrophobicity is a vital parameter in surficial property as reaction in aqueous solution(H. Li et al., 2021), especially the waste treatment, and catalysis. Therefore, an effective depressant for talc needs to be added into the system of talc/sulfide minerals.

Previous research presented that polysaccharide depressants could adsorb on talc surface and the surface of it alters to hydrophily(Feng et al., 2018). Polysaccharides are considered as a polymer of high molecular weights which composed of at least ten monosaccharides(Wu et al., 2022). Many different types of polysaccharides are naturally found. Such as starch, cellulose, guar gum and glycogen(Jenkins and Ralston, 1998). However, only a few numbers of them can be directly used in minerals flotation due to its molecular structure properties or/and high price. Thus, to achieve the polysaccharides selectively absorb on talc surface, polysaccharides need to be modified. So far, carboxymethyl cellulose (CMC) is confirmed to be an effective depressant for talc as well as other gangue minerals in real ore flotation(Shortridge et al., 2000; Liu et al., 2006; Parolis et al., 2008).

CMC is obtained by the carboxymethylation of cellulose which widely used in petroleum, food, medicine, textile, and papermaking industries due to that the aqueous solution of has the functions of thickening, film forming, bonding, water retention and colloid protection(Hosseini et al., 2022; Yildirim-Yalcin et al., 2022; Zhang et al., 2023). Many investigations indicated the adsorption behavior of CMC on talc though multiple measurements, such as zeta potential, atom force microscope and X-ray photoelectron spectroscopy(Jin et al., 2018; C. Li et al., 2021a), which revealed the interaction between the CMC and talc surface to some extent, including hydrogen bond, hydrophobic bonding, and chemical adsorption. However, few studies have been conducted concerning the microscopic interaction mechanism of basal face/edge face with CMC, causing the difference of adsorption conclusions. Hence, the interaction of CMC with talc is still a controversial issue.

In recent years, with the development of quantum chemistry, it is feasible to study the interaction between reagents and solid surface at the atom/molecular scale, DFT calculation has been considered as an effective quantum chemical method to study the reagent molecules properties, minerals surface activation, and the adsorption form between reagents and minerals surface which offers a better understanding of the reacted mechanism on mineral surface(Liu et al., 2020, 2021; Zhan et al., 2020; Cui and Chen, 2021; Luo et al., 2022a). MDs was a useful tool for investigating static and dynamic properties of molecules from interactions between reagents and solid surface in a molecular level(Yuan et al., 2018; Bhatt et al., 2023; Gomez de Santos et al., 2023). It is worth noting that the physical or/and chemical adsorption process and nature of CMC on the talc surface cannot be clearly understood in flotation process. Therefore, in this study, a combined MDs and DFT calculations was introduced to deeply understand the reaction process and mechanism of CMC with talc surface.

2. Computational methods and details

2.1. Molecular dynamic simulations (MDs)

2.1.1. Model construction

Firstly, the simulation model was constructed. Talc (001) and talc (100) plane were selected to study the interaction between CMC and basal face/edge face of talc. The parameters about talc crystal were as follows: C2, a = 0.526 nm, b = 0.91 nm, c = 1.881 nm, and $\alpha = \gamma = 90^{\circ}$, $\beta = 100^{\circ}$(Luo et al., 2022b). Type of water molecules used in the simulation was SPC model(Du and Miller, 2007). The illustration for model construction was shown in Fig. 1. 500 water molecules and CMC were constructed by amorphous cell. Subsequently, based on cleave surface and supercell model, the basal plane and edge plane of talc were constructed. Lastly, the talc (001) and (100) crystal plane and CMC aqueous solutions layer were built through the Build Layer module. The distance between aqueous solutions and plane of talc was ~3 Å. Enough vacuum space of 20 Å was chosen along the z-direction of simulation box with the aim of avoiding the influence of periodic boundary condition (Luo et al., 2022b).

2.1.2. Computational parameters

MDs was carried out using Materials Studio 2018 to determine the interaction of CMC and Talc in aqueous solutions. The program was useful for testing the conformational and vibrational information of atoms in isolated system(Atluri et al., 2018). Here, CLAYFF force field (Cygan et al., 2004), the ab initio force field, based on nonbonded description of interaction with hydrated phases, was applied on the geometric optimization and MDs, and the parameters was shown in Table 1. CLAYFF force field was successfully proved for simulating the water molecules on clay mineral systems in the field of environmental and material science(Chen et al., 2023a). NVT ensemble with constant particle number, volume, and temperature at 298 K during the simulations was performed during MDs because of no disturbance to trajectory. As for temperature, it was regulated by the Nose thermostat method in MDs. Maxwell-Boltzmann distribution was used to describe the randomly initial velocity. 500 ps was used to make the system

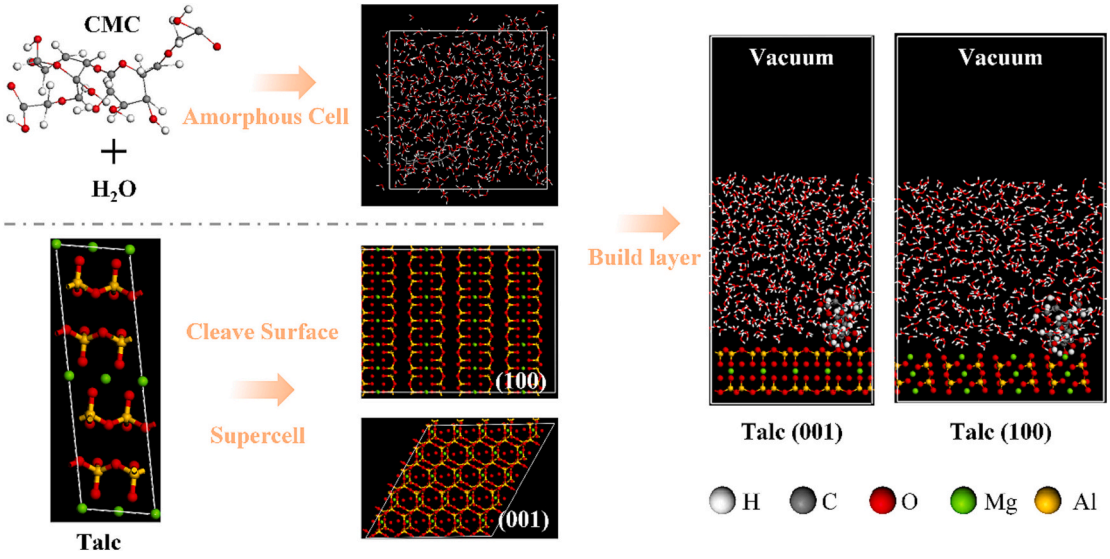

Fig. 1. The illustration for model construction about the interaction of CMC with talc (001) and talc (100) plane in aqueous solutions.

Table 1
Parameters for CLAYFF force field used in the work.

Species	Symbol	Charge (e)	R_0 (Å)
Water hydrogen	h*	0.4100	
Hydroxyl hydrogen	ho	0.4250	
Water oxygen	o*	−0.8200	3.5532
Hydroxyl oxygen	oh	−0.9500	3.5532
Bridging oxygen with tetrahedral substitution	obts	−1.1688	3.5532
Hydroxyl oxygen with substitution	ohs	−1.0808	3.5532
Tetrahedral silicon	st	2.1000	3.7064
Octahedral magnesium	mgo	1.3600	5.9090

equilibrated, and time step of 0.001 ps was set. In the x, y and z direction, Periodic boundary conditions were put. During the simulation process, Van der waals forces with a cutoff distance of 12.5 Å and electrostatic interaction were described by atom-based method and Ewald method, respectively.

2.2. DFT calculation

Detailed surface interaction was investigated by DFT as implemented in DMol3 package. A 2 × 2 × 1 supercell of talc(001) and talc(100) was applied for studying the interaction property. Exchange was described by Perdew-Bruke-Ernzerhof (PBE) functional within generalized gradient approximation (GGA). A slab model with 20 Å vacuum layer along z- axis was adopted to avoid self-interaction. Cutoff energy was set as 450 eV, and k-point was selected as fine precision.

3. Results and discussion

3.1. Equilibration

Fluctuation curves, was commonly utilized to evaluate the MDs system's equilibrium state. As shown in Fig. 2, equilibrium in talc(001) and talc(100) were achieved when the range of fluctuation in energy falls within the range of error allowable. Thus, these demonstrated the equilibration phase of simulation in terms of energy and the reliability of used last 500 frames for analysis had been achieved.

3.2. Adsorption configuration

Adsorption configuration of CMC on the talc(001) and talc(100) was exhibited in Fig. 3a and Fig. 3b. CMC was absorbed on the talc(001) and talc(100), indicating that there is an attraction between CMC molecule and the surface of Talc. Water molecules were closer to the talc(100) than talc(001) owing to the hydrophilic property of edge of Talc. Talc (001) with nonpolar structure of siloxane was hydrophobic, showing weak electron donors to water molecules(Zbik and Smart, 2002). As for talc(100), the edge surface with hydroxyl group was prone to adsorb water molecules. By looking into the distribution of water molecules over time in the system of talc(001) and talc(100), mean square displacement (MSD) was calculated as following equation:

$$MSD = \left\langle \left| x(t) - x_0 \right|^2 \right\rangle = \frac{1}{N} \sum_{i=1}^{N} \left| x^{(i)}(t) - x^{(i)}(0) \right|^2 \quad (1)$$

Where N meant the number of averaged particles; In which vector $x^{(i)}(0) = x_0{}^{(i)}$ and $x^{(i)}(t)$ presented the reference position and position at time t of the *i-th* particle, respectively.

Based on the derivation of equation for n-dimensions, the relation between running diffusion constant (D_a) and MSD could be calculated as follows:

$$D_a = \frac{1}{6t} MSD \quad (2)$$

Thus, the slope of MSD curve was positively related to the running diffusion constant (Fig. 3c). Higher running diffusion constant of water molecules on talc(001) than that on talc(100) demonstrated the easier stabilization of water molecules on talc(100). The adsorbed water molecules were prone to drag CMC get close to surface of talc(100), enhancing the binding energy of CMC and edge.

3.3. Interfacial hydration layer

In order to study the water molecules configuration on the basal plane and edge plane of talc, the relative concentration distribution of interfacial water with distace from the talc(001) and talc(100) surface was showed in Fig. 4c. Assessment of water molecules concentration was beneficial for detecting the thickness and structure of hydration layer.

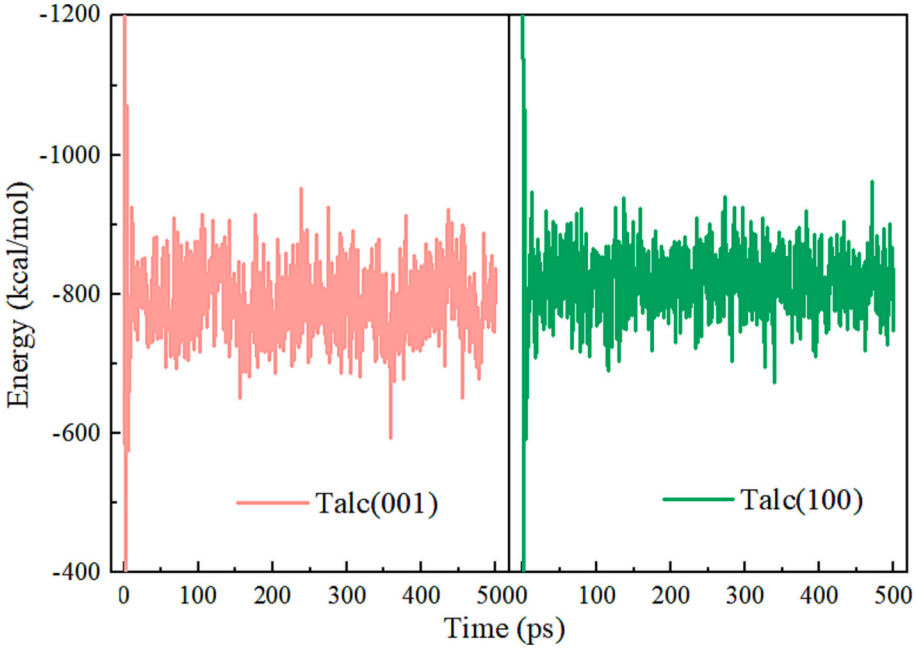

Fig. 2. Fluctuation curves of energy in the MDS system about CMC aqueous solutions in talc(001) and talc(100).

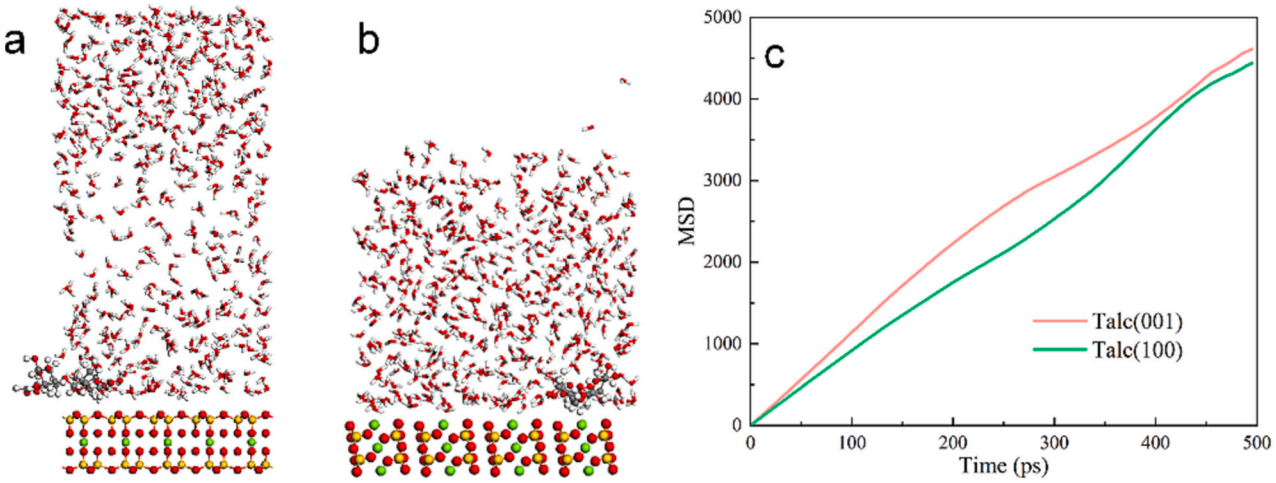

Fig. 3. The model of CMC on the surface of (a) talc(001) and (b) talc(100) in aqueous solutions after structure optimization. (c) MSD curve of water molecules on the surface of talc(001) and talc(100) as a function of time.

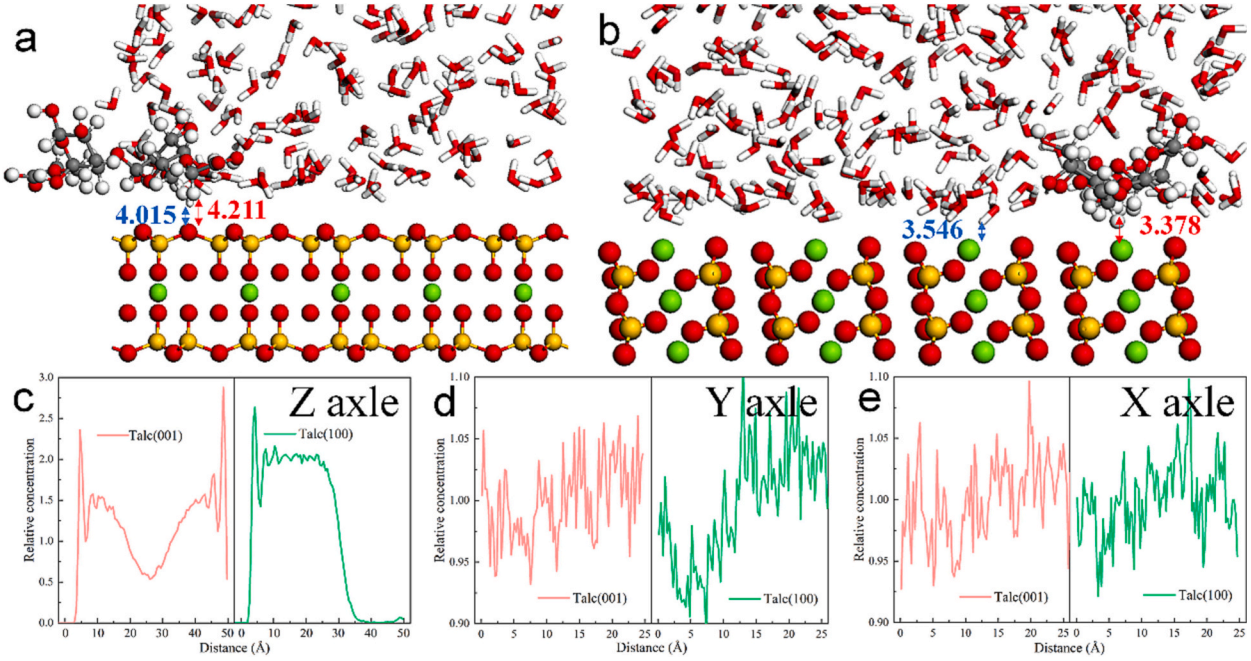

Fig. 4. The picture of (a) CMC and talc(001), (b) CMC and talc(100) in aqueous solutions including the distance. The relative concentration distribution of interfacial water with distance from talc(001) and talc(100) in the view of (c) x, (d) y, and (e) z axle.

Peaks in the water molecules distribution could be observed, and it meant the water molecules layer. There are around three water molecules layers at the basal plane and edge plane of talc. Interestingly, the relative concentration of hydration layer on the surface of talc(100) was higher than that on the surface of talc(001), which was resulted from the stronger attraction of water molecules on the surface of talc(100). Therefore, most of water molecules focused on the distribution nearby the surface of talc(100). Further, relative concentration of water molecules from other sides was displayed in Fig. 4d and Fig. 4e. From the view of y and z axis, relative concentration of water molecules on talc (001) was almost uniform distributed, while there was a peak on talc (001) due to the strong interaction of CMC and water molecule, as displayed in Fig. 4a and Fig. 4b. Red color was the distance of CMC and talc surface, while blue color meant the distance between water molecules and talc surface. Distance between water molecules and talc(100) was closer to that between water molecules and talc(001), displaying that higher interaction of water molecules and edge. The same results of stronger interaction of CMC on the edge surface of talc could be obtained.

3.4. Adsorption energy

In general, adsorption energy revealed an insight into the interaction among CMC, water molecules and talc, thus the interaction of CMC and the basal plane, edge plane of Talc in water system was calculated. The adsorption energy of talc/H_2O, talc/CMC and CMC/H_2O was calculated according to following equations:

$$\Delta E_{Talc/H_2O} = E_{Talc/H_2O} - E_{Talc} - E_{H_2O} \quad (3)$$

$$\Delta E_{Talc/CMC} = E_{Talc/CMC} - E_{Talc} - E_{CMC} \quad (4)$$

$$\Delta E_{CMC/H_2O} = E_{CMC/H_2O} - E_{CMC} - E_{H_2O} \quad (5)$$

Where $\Delta E_{Talc/H_2O}$, $\Delta E_{Talc/CMC}$ and $\Delta E_{CMC/H_2O}$ were the adsorption energy of talc and water molecules, talc and CMC, CMC and water molecules, respectively; E_{Talc/H_2O}, $E_{Talc/CMC}$, E_{CMC/H_2O}, E_{Talc}, E_{H_2O} and E_{CMC} were the energy of talc/H_2O, talc/CMC and CMC/H_2O system, respectively.

As exhibited in Fig. 5a, talc had an affinity with water molecules and CMC. More negative adsorption energy expressed stronger interaction. Water molecules showed more affinity with talc(100) than talc(001) because of the polar group on the edge plane of talc. According to the theory of induction force, talc(001) would bind strongly with water molecules. In the similar principle, there is a higher interaction between CMC and talc(100) than CMC and talc(001). Except this, the enhanced interaction could be ascribed to the stronger interaction between talc (100) and water molecules. CMC showed higher binding strength between water molecules in talc(100) system, compared with in talc(001) system. The strong affinity was originated from the dragged water molecules to the surface of talc(100). Besides, the phenomenon was demonstrated by radial distribution function (RDF) in Fig. 5b. RDF was calculated as:

$$\rho g(r) 4\pi r^3 = dN \tag{6}$$

Where ρ represented the density of system.

Based on the results of RDF, the distribution of water molecules around CMC could be obtained. In comparison with in talc(001) system, there are higher peak position in talc(100) system, which revealed that CMC got closer to water molecules on the surface of talc(100). In conclusion, as CMC closed to the surface of talc(100) by with dragged water molecules, CMC could bind tightly with water molecules and talc (100).

3.5. Bonding and charge transfer

With the aim of further revealing interaction states and charge transfer, electron density difference, partial density of states (PDOS), and Mulliken atomic charge changes (ΔQ) were calculated. Fig. 6 presented the electron density difference after adsorption of CMC on the surface of basal and edge plane of talc. It could be observed that electrons overlap in blue color of H atoms in CMC and O atoms in talc, O atoms in CMC and O, Si atoms in talc, indicating the bonding and electron transfer of CMC and talc. Besides, the degree of overlap of CMC and talc(100) (Fig. 6b) was greater than that of CMC and talc(001) (Fig. 6a), which indicated that stronger interaction between CMC and edge plane of talc. The tight bonding between CMC and talc(100) might resulted from the unsaturated and active O atoms in edge planes.

Interacted orbitals between CMC and talc(110) was studied for clarifying the insight interaction. The PDOS of H, O atoms in CMC, and O, Si, Mg in talc was presented to compare the bonding orbitals as shown in Fig. 7. H *s* orbital in CMC overlapped with O *s*, *p* orbitals in talc(100)

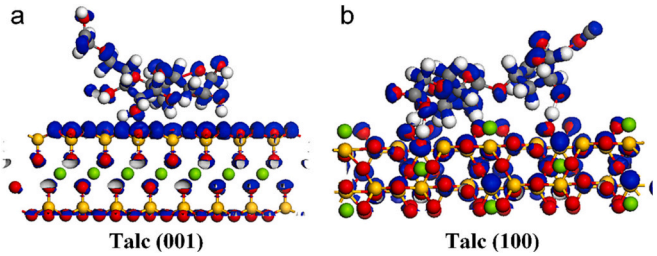

Fig. 6. Electron density difference of CMC on the surface of (a) basal and (b) edge plane of talc.

in the energy range from −22.5 to −17.5 eV and − 10 eV to 0 eV (Fig. 7a). The overlaps indicated the strong interaction between H atoms in CMC and O atoms in talc(100). As for the O atoms in CMC structure, they bound with Si atoms or Mg atoms in the structure of talc(100). As depicted in Fig. 7b, there are overlaps of O *s*, *p* orbitals in CMC, Si *s*, *p* orbitals, and Mg *s*, *p* orbitals in the range of −22.5 to −17.5 eV and − 10 eV to 0 eV. The overlap degree of O orbital and Si orbital was bigger than that of O orbital and Mg orbital, which demonstrated the stronger interaction between O atoms and Si atoms on the surface of talc(100).

Mulliken atomic charge changes of H, O atoms in CMC, and O (marked as O_s for distinguishing), Si and Mg atoms in talc before and after the adsorption were calculated, as shown in Fig. 8. It was found that the major lost charges of O atoms in CMC transferred to the nearby Si and Mg atoms in talc, while H atoms in CMC gained charges which from O_s atoms in talc. The phenomenon indicated that the interaction between H atoms in CMC and O atoms in talc, and O atoms in CMC and Si, Mg atoms in talc, which was in line with the results of electron density difference and PDOS, which might be resulted from the polar group in edge plane of talc. Interestingly, in talc(100), Mg atoms acted as electron acceptance for the enhanced interaction. Thus, the interaction between CMC and edge plane was stronger than that between CMC and basal plane.

Given the above results, it demonstrated that CMC bind stronger with edge plane than that with basal plane of talc. Through the MDs and DFT calculation, it was found that enhanced adsorption of CMC on the edge surface of talc was owing to strengthened interaction of polar group with CMC. Besides, the hydration shell played an important role during the adsorption. Dragged water molecules close to surface of edge would improve the adsorption of CMC. As a consequence, it is reasonable that if symmetrical structure of basial surface property was modified, and it would be beneficial for the separation of talc with other minerals by adding CMC in the flotation. These methods and discovery may have enormous potential application in surface structure modification about catalysis, waste treatment.

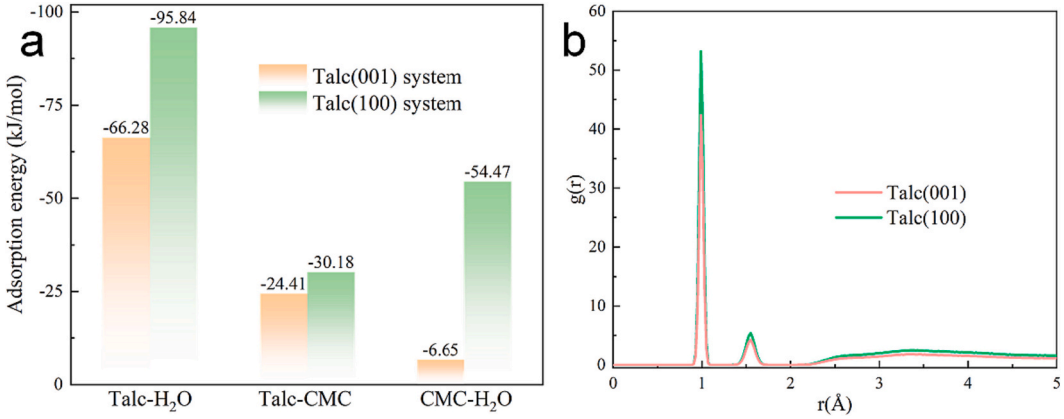

Fig. 5. (a) Adsorption energy of Talc/H_2O, Talc/CMC and CMC/H_2O in the system of talc(001) and talc(100). (b) RDF of water molecules distribution around CMC.

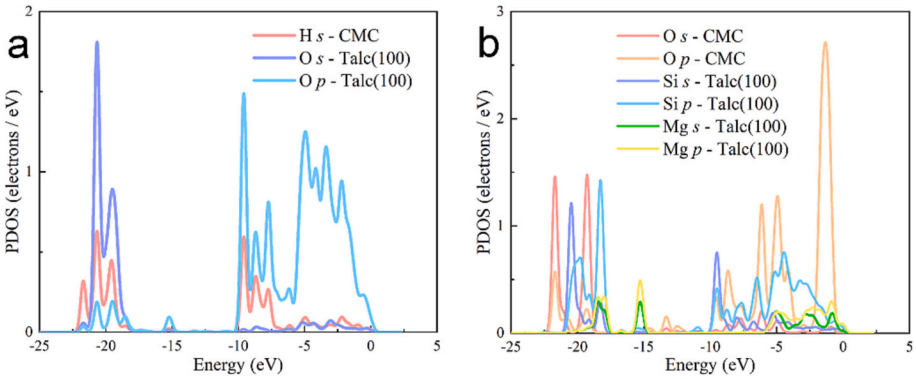

Fig. 7. (a) PDOS of H *s* orbital in CMC, O *s*, *p* orbitals in talc(100); (b) PDOS of O *s*, p orbitals in CMC, and Si *s*, *p* orbitals, Mg *s*, *p* orbitals in talc(100).

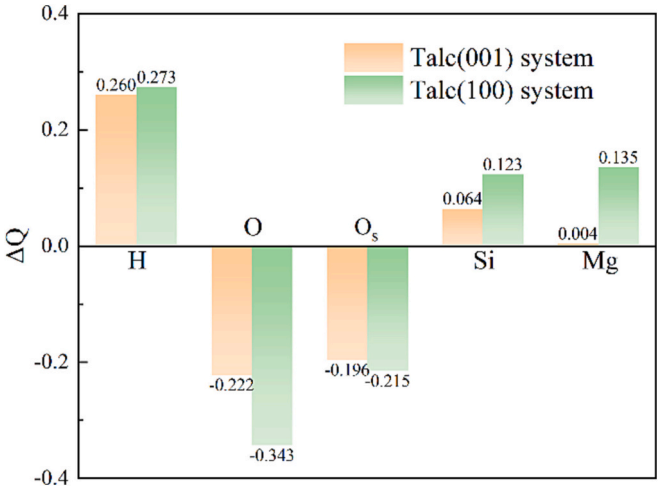

Fig. 8. Mulliken atomic charge changes of H, O atoms in CMC and O (O_s), Si, Mg atoms in talc before and after adsorption on the surface of talc.

4. Conclusion

In summary, the interaction of CMC with basal and edge plane was well studied based on MDs and DFT. The adsorption energy of CMC on the surface of basal plane of talc was smaller than that on the surface of edge plane. The results were ascribed to the enhanced interaction of polar group on the edge plane and the dragged water molecules. There were interactions between H atom in CMC and O atom in edge plane, between O atom in CMC and Si, Mg atoms in edge plane. Polar O atoms and Mg atoms in the edge plane strengthen the binding between CMC and talc. Furthermore, owing to the strong adsorption of water molecules on the surface of edge plane, the adsorbed CMC with water molecules together would bind with edge plane. In addition, the hydration shell on the surface of basal and edge plane of talc would be affected by CMC. High concentration of water molecules in the order layer appeared on the surface of edge plane. The method used in the work gave a new insight to investigate adsorption of hydrophilic reagents on surface of mineral from hydration view and interaction. This study clearly showed the interaction of CMC of basal and edge plane of talc from the molecule levels, and it could guide the application of talc in adsorption of heavy metal ions and dyes for water treatment.

CRediT authorship contribution statement

Weiquan Zhan: Writing – original draft, Methodology, Formal analysis, Investigation. **Siyuan Yang:** Investigation, Methodology. **Shenxu Bao:** Formal analysis, Methodology. **Liuyi Ren:** Software, Investigation. **Cheng Liu:** Writing – review & editing, Data curation.

Declaration of Competing Interest

The authors declare that they have no known competing financial interests or personal relationships that could have appeared to influence the work reported in this paper.

Data availability

Data will be made available on request.

Acknowledgement

The authors acknowledge the support of National Natural Science Foundation of China (No. 52274269), the National Key Research and Development Program of China (No. 2022YFC2905800). Zhan gratefully acknowledges the Consejo Nacional de Ciencia y Tecnología (CONACYT) of Mexico for offering him the scholarship under the grant No. 813934 during his Ph.D. studies.

References

Atluri, V., Jin, J., Shrimali, K., Dang, L., Wang, X., Miller, J.D., 2018. The hydrophobic surface state of talc as influenced by aluminum substitution in the tetrahedral layer. J. Colloid Interface Sci. 536, 737–748. https://doi.org/10.1016/j.jcis.2018.10.085.

Bhatt, P., Bhatt, K., Chen, W.J., Huang, Y., Xiao, Y., Wu, S., Lei, Q., Zhong, J., Zhu, X., Chen, S., 2023. Bioremediation potential of laccase for catalysis of glyphosate, isoproturon, lignin, and parathion: Molecular docking, dynamics, and simulation. J. Hazard. Mater. 443, 130319 https://doi.org/10.1016/J.JHAZMAT.2022.130319.

Burkett, S.L., Maumbe, W.V., Lin, S., 2022. Reconsideration of the structure of magnesium n-hexadecylsilicate and other "talc-like" layered magnesium organosilicates. Appl. Clay Sci. 216, 106364 https://doi.org/10.1016/J.CLAY.2021.106364.

Chen, Y., Wen, L., Chen, J., Luo, H., Liu, J., 2022. In situ growth of g-C_3N_4 on clay minerals of kaolinite, sepiolite, and talc for enhanced solar photocatalytic energy conversion. Appl. Clay Sci. 216, 106337 https://doi.org/10.1016/J.CLAY.2021.106337.

Chen, J., Chu, X., Cheng, Y., Shu, Q., Ling, Y., Shang, H., Min, F., 2023a. Application of molecular dynamics simulations in interface interaction of clay: current status and perspectives. Asia Pac. J. Chem. Eng. e2955 https://doi.org/10.1002/APJ.2955.

Chen, S., Zhang, M., Chen, H., Fang, Y., 2023b. Removal of methylene blue from aqueous solutions by surface modified talc. Materials 16, 3597. https://doi.org/10.3390/MA16093597.

Cui, W., Chen, J., 2021. Insight into mineral flotation fundamentals through the DFT method. Int. J. Min. Sci. Technol. 31, 983–994. https://doi.org/10.1016/J.IJMST.2021.10.001.

Cygan, R.T., Liang, J.J., Kalinichev, A.G., 2004. Molecular models of hydroxide, oxyhydroxide, and clay phases and the development of a general force field. J. Phys. Chem. B 108, 1255–1266. https://doi.org/10.1021/JP0363287.

Dias, G., Prado, M., Le Roux, C., Poirier, M., Micoud, P., Ligabue, R., Martin, F., Einloft, S., 2020. Synthetic talc as catalyst and filler for waterborne polyurethane-based nanocomposite synthesis. Polym. Bull. 77, 975–987. https://doi.org/10.1007/S00289-019-02789-W/TABLES/3.

Du, H., Miller, J.D., 2007. Adsorption states of amphipatic solutes at the surface of naturally hydrophobic minerals: a molecular dynamics simulation study. Langmuir 23, 11587–11596. https://doi.org/10.1021/LA701604U.

Feng, B., Peng, J., Zhang, Wenpu, Ning, X., Guo, Y., Zhang, Wencai, 2018. Use of locust bean gum in flotation separation of chalcopyrite and talc. Miner. Eng. 122, 79–83. https://doi.org/10.1016/J.MINENG.2018.03.044.

Fuerstenau, M.C., Lopez-Valdivieso, A., Fuerstenau, D.W., 1988. Role of hydrolyzed cations in the natural hydrophobicity of talc. Int. J. Miner. Process. 23, 161–170. https://doi.org/10.1016/0301-7516(88)90012-9.

Gomez de Santos, P., González-Benjumea, A., Fernandez-Garcia, A., Aranda, C., Wu, Y., But, A., Molina-Espeja, P., Maté, D.M., Gonzalez-Perez, D., Zhang, W., Kiebist, J., Scheibner, K., Hofrichter, M., Świderek, K., Moliner, V., Sanz-Aparicio, J., Hollmann, F., Gutiérrez, A., Alcalde, M., 2023. Engineering a highly regioselective fungal peroxygenase for the synthesis of hydroxy fatty acids. Angewandte Chemie-International Edition 62, e202217372. https://doi.org/10.1002/ANIE.202217372.

Hosseini, H., Zirakjou, A., McClements, D.J., Goodarzi, V., Chen, W.H., 2022. Removal of methylene blue from wastewater using ternary nanocomposite aerogel systems: Carboxymethyl cellulose grafted by polyacrylic acid and decorated with graphene oxide. J. Hazard. Mater. 421, 126752 https://doi.org/10.1016/J.JHAZMAT.2021.126752.

Jenkins, P., Ralston, J., 1998. The adsorption of a polysaccharide at the talc–aqueous solution interface. Colloids Surf. A Physicochem. Eng. Asp. 139, 27–40. https://doi.org/10.1016/S0927-7757(98)00217-9.

Jin, S., Shi, Q., Li, Q., Ou, L., Ouyang, K., 2018. Effect of calcium ionic concentrations on the adsorption of carboxymethyl cellulose onto talc surface: flotation, adsorption and AFM imaging study. Powder Technol. 331, 155–161. https://doi.org/10.1016/J.POWTEC.2018.03.014.

Khraisheh, M., Holland, C., Creany, C., Harris, P., Parolis, L., 2005. Effect of molecular weight and concentration on the adsorption of CMC onto talc at different ionic strengths. Int. J. Miner. Process. 75, 197–206. https://doi.org/10.1016/J.MINPRO.2004.08.012.

Li, H., Yang, W., Wu, C., Xu, J., 2021. Origin of the hydrophobicity of sulfur-containing iron surfaces. Phys. Chem. Chem. Phys. 23, 13971–13976. https://doi.org/10.1039/D1CP00588J.

Li, C., Shi, Q., Zhang, G., Liu, H., Feng, H., 2021a. Effect of aluminum ions on the adsorption of carboxymethyl cellulose onto talc. Miner. Eng. 170, 107018 https://doi.org/10.1016/J.MINENG.2021.107018.

Li, C., Zhang, G., Xun, L., Liu, H., Shi, Q., 2021b. Flotation separation of molybdenite from talc using a new inhibitor Artemisia sphaerocephala Krasch gum. Miner. Eng. 174, 107227 https://doi.org/10.1016/J.MINENG.2021.107227.

Li, B., Shi, Q., Miao, B., Liu, D., Jin, S., Wang, Z., 2023. Application of exopolysaccharide directionally synthesized by Xanthomonas campestris as the green selective depressant for the clean flotation of talc: statistical optimization and mechanism analysis. J. Clean. Prod. 383, 135381 https://doi.org/10.1016/J.JCLEPRO.2022.135381.

Liu, G., Feng, Q., Ou, L., Lu, Y., Zhang, G., 2006. Adsorption of polysaccharide onto talc. Miner. Eng. 19, 147–153. https://doi.org/10.1016/J.MINENG.2005.08.005.

Liu, J., Miller, J.D., Yin, X., Gupta, V., Wang, X., 2014. Influence of ionic strength on the surface charge and interaction of layered silicate particles. J. Colloid Interface Sci. 432, 270–277. https://doi.org/10.1016/j.jcis.2014.06.028.

Liu, M., Chen, J., Chen, Y., Zhu, Y., 2020. Interaction between smithsonite and carboxyl collectors with different molecular structure in the presence of water: a theoretical and experimental study. Appl. Surf. Sci. 510, 145410 https://doi.org/10.1016/J.APSUSC.2020.145410.

Liu, C., Zheng, Y., Yang, S., Fu, W., Chen, X., 2021. Exploration of a novel depressant polyepoxysuccinic acid for the flotation separation of pentlandite from lizardite slimes. Appl. Clay Sci. 202, 105939 https://doi.org/10.1016/J.CLAY.2020.105939.

Long, T., Zhao, H., Wang, Y., Yang, W., Deng, S., Xiao, W., Lan, X., Wang, Q., 2022. Synergistic mechanism of acidified water glass and carboxymethyl cellulose in flotation of nickel sulfide ore. Miner. Eng. 181, 107547 https://doi.org/10.1016/J.MINENG.2022.107547.

Luo, Y., Ou, L., Chen, J., Zhang, G., Xia, Y., Zhu, B., Zhou, H., 2022a. Insights into the adsorption performance and mechanism of hydrated ca ion on talc (001) basal surface from DFT calculation. Int. J. Min. Sci. Technol. 32, 887–896. https://doi.org/10.1016/J.IJMST.2022.05.007.

Luo, Y., Ou, L., Chen, J., Zhou, H., Yin, C., Yang, H., 2022b. Insights into the adsorption mechanism of water at different coverage rates on talc ($Mg_3Si_4O_{10}(OH)_2$) (001) basal surface: a first-principles study. J. Mol. Liq. 363, 119879 https://doi.org/10.1016/J.MOLLIQ.2022.119879.

Maleki, H., Kazemeini, M., Bastan, F., 2017. Transesterification of canola oil to biodiesel using CaO/Talc nanopowder as a mixed oxide catalyst. Chem. Eng. Technol. 40, 1923–1930. https://doi.org/10.1002/CEAT.201600579.

Mälhammar, G., 1990. Determination of some surface properties of talc. Colloids Surf. A Physicochem. Eng. Asp. 44, 61–69. https://doi.org/10.1016/0166-6622(90)80187-9.

Morris, G.E., Fornasiero, D., Ralston, J., 2002. Polymer depressants at the talc–water interface: adsorption isotherm, microflotation and electrokinetic studies. Int. J. Miner. Process. 67, 211–227. https://doi.org/10.1016/S0301-7516(02)00048-0.

Parolis, L.A.S., van der Merwe, R., Groenmeyer, G.V., Harris, P.J., 2008. The influence of metal cations on the behaviour of carboxymethyl celluloses as talc depressants. Colloids Surf. A Physicochem. Eng. Asp. 317, 109–115. https://doi.org/10.1016/J.COLSURFA.2007.10.001.

Shortridge, P.G., Harris, P.J., Bradshaw, D.J., Koopal, L.K., 2000. The effect of chemical composition and molecular weight of polysaccharide depressants on the flotation of talc. Int. J. Miner. Process. 59, 215–224. https://doi.org/10.1016/S0301-7516(99)00077-0.

Sprynskyy, M., Kowalkowski, T., Tutu, H., Cukrowska, E.M., Buszewski, B., 2011. Adsorption performance of talc for uranium removal from aqueous solution. Chem. Eng. J. 171, 1185–1193. https://doi.org/10.1016/J.CEJ.2011.05.022.

Wu, W., Chen, T., Shao, Y., Ye, G., Tong, X., 2022. The flotation separation of molybdenite from talc using zinc sulfate in sodium silicate system and related mechanism. Colloids Surf. A Physicochem. Eng. Asp. 641, 128451 https://doi.org/10.1016/J.COLSURFA.2022.128451.

Xian, Y., Hong, Y., Li, Y., Li, X., Zhang, S., Chen, L., 2022. Pulsating high-gradient magnetic separation of chalcopyrite and talc. Miner. Eng. 178, 107410 https://doi.org/10.1016/J.MINENG.2022.107410.

Yan, L., Masliyah, J.H., Xu, Z., 2013. Interaction of divalent cations with basal planes and edge surfaces of phyllosilicate minerals: Muscovite and talc. J. Colloid Interface Sci. 404, 183–191. https://doi.org/10.1016/J.JCIS.2013.04.023.

Yildirim-Yalcin, M., Tornuk, F., Toker, O.S., 2022. Recent advances in the improvement of carboxymethyl cellulose-based edible films. Trends Food Sci. Technol. 129, 179–193. https://doi.org/10.1016/J.TIFS.2022.09.022.

Yuan, Y., Zhan, W., Yi, H., Zhao, Y., Song, S., 2018. Molecular dynamics simulations study for the effect of cations hydration on the surface tension of the electrolyte solutions. Colloids Surf. A Physicochem. Eng. Asp. 539, 80–84. https://doi.org/10.1016/J.COLSURFA.2017.12.005.

Zafari, S., Ghorbani-Vaghei, R., Alavinia, S., 2021. Poly(sulfonamide-thiourea) grafted γ-Fe_2O_3@talc as a green catalyst for the synthesis of substituted tetrahydropyridines. Mater. Chem. Phys. 270, 124840 https://doi.org/10.1016/j.matchemphys.2021.124840.

Zbik, M., Smart, R.S.C., 2002. Dispersion of kaolinite and talc in aqueous solution: nano-morphology and nano-bubble entrapment. Miner. Eng. 15, 277–286. https://doi.org/10.1016/S0892-6875(02)00034-1.

Zeitler, T.R., Greathouse, J.A., Gale, J.D., Cygan, R.T., 2014. Vibrational analysis of brucite surfaces and the development of an improved force field for molecular simulation of interfaces. J. Phys. Chem. C 118, 7946–7953. https://doi.org/10.1021/JP411092B.

Zhan, W., Yi, H., Song, S., Zhao, Y., Rao, F., 2019. Hydrophobic agglomeration behaviors of clay minerals as affected by siloxane structure. Colloids Surf. A Physicochem. Eng. Asp. 568, 36–42. https://doi.org/10.1016/J.COLSURFA.2019.01.061.

Zhan, W., Jia, F., Yuan, Y., Liu, C., Sun, K., Yang, B., Song, S., 2020. Controllable incorporation of oxygen in MoS_2 for efficient adsorption of Hg^{2+} in aqueous solutions. J. Hazard. Mater. 384, 121382 https://doi.org/10.1016/J.JHAZMAT.2019.121382.

Zhang, W., Li, W., Li, S., 2023. Molten salt assisted self-activated carbon with controllable architecture for aqueous supercapacitor. J. Mater. Sci. Technol. 156, 107–117. https://doi.org/10.1016/j.jmst.2022.12.079.

Zhao, K., Wang, X., Wang, Z., Yan, W., Zhou, X., Xu, L., Wang, C., 2019. A novel depressant for selective flotation separation of pyrite and pyrophyllite. Appl. Surf. Sci. 487, 9–16. https://doi.org/10.1016/J.APSUSC.2019.04.252.

Zhong, C., Wang, H., Zhang, L., Guo, M., Feng, B., 2021. Flotation separation of molybdenite and talc by xanthan gum. Powder Technol. 388, 158–165. https://doi.org/10.1016/J.POWTEC.2021.04.080.